Inter-annual and inter-seasonal variability of the Orkney wave power resource

Neill, S.P.; Lewis, M.J.; Hashemi, M.R.; Slater, E.; Lawrence, J.; Spall, S.A.

Applied Energy

DOI:
10.1016/j.apenergy.2014.07.023

Published: 01/08/2014

Publisher's PDF, also known as Version of record

Applied Energy 132 (2014) 339–348

Contents lists available at ScienceDirect

Applied Energy

journal homepage: www.elsevier.com/locate/apenergy

Inter-annual and inter-seasonal variability of the Orkney wave power resource

Simon P. Neill [a,*], Matt J. Lewis [a], M. Reza Hashemi [a], Emma Slater [b], John Lawrence [c], Steven A. Spall [d]

[a] School of Ocean Sciences, Bangor University, Menai Bridge LL59 5AB, UK
[b] British Oceanographic Data Centre, Joseph Proudman Building, 6 Brownlow Street, Liverpool L3 5DA, UK
[c] The European Marine Energy Centre (EMEC) Ltd., Old Academy, Stromness KW16 3AW, UK
[d] Xodus Group, Cefn-y-Borth, Rhoscolyn, Holyhead LL65 2EQ, UK

HIGHLIGHTS

- We ran high resolution wave model simulations for Orkney and the Pentland Firth.
- We resolve inter-annual variability in the wave resource over a 10 year period.
- We quantify regional uncertainty in the Orkney wave resource.
- Our wave resource estimates correlate well with the NAO over winter months.
- There is less winter variability in the practical *versus* theoretical resource.

ARTICLE INFO

Article history:
Received 20 January 2014
Received in revised form 6 June 2014
Accepted 8 July 2014
Available online 1 August 2014

Keywords:
Wave power
Wave resource
SWAN wave model
Inter-annual variability
North Atlantic Oscillation
Orkney

ABSTRACT

The waters surrounding the Orkney archipelago in the north of Scotland are one of the key regions in the world suitable for exploitation of both wave and tidal energy resources. Accordingly, Orkney waters are currently host to 1.08 GW of UK Crown Estate leased wave and tidal energy projects, with a further 0.5 GW leased in the southern part of the adjacent Pentland Firth. Although several wave resource models exist of the region, most of these models are commercial, and hence the results not publicly available, or have insufficient spatial/temporal resolution to accurately quantify the wave power resource of the region. In particular, no study has satisfactorily resolved the inter-annual and inter-seasonal variability of the wave resource around Orkney. Here, the SWAN wave model was run at high resolution on a high performance computing system, quantifying the Orkney wave power resource over a ten year period (2003–2012), a decade which witnessed considerable inter-annual variability in the wave climate. The results of the validated wave model demonstrate that there is considerable variability of the wave resource surrounding Orkney, with an extended winter (December–January–February–March, DJFM) mean wave power ranging from 10 to 25 kW/m over the decade of our study. Further, the results demonstrate that there is considerably less uncertainty (30%) in the high energy region to the west of Orkney during winter months, in contrast to much greater uncertainty (60%) in the lower energy region to the east of Orkney. The DJFM wave resource to the west of Orkney correlated well with the DJFM North Atlantic Oscillation (NAO). Although a longer simulated time period would be required to fully resolve inter-decadal variability, these preliminary results demonstrate that due to considerable inter-annual variability in the NAO, it is important to carefully consider the time period used to quantify the wave power resource of Orkney, or regions with similar exposure to the North Atlantic. Finally, our study reveals that there is significantly less variability in the practical wave power resource, since much of the variability in the theoretical resource is contained within relatively few extreme events, when a wave device enters survival mode.

1. Introduction

The global wave power resource has been estimated as around 2.1 TW [1], with many regions of the northwest European shelf seas that are exposed to the North Atlantic containing an annual mean wave power in excess of 20 kW/m [2]. However, this region

* Corresponding author.
E-mail address: s.p.neill@bangor.ac.uk (S.P. Neill).

http://dx.doi.org/10.1016/j.apenergy.2014.07.023
0306-2619/

experiences considerable inter-annual and inter-seasonal variability of the wave power resource [3], and this uncertainty is one of the factors that is slowing down the progression of full-scale prototypes and pre-commercial devices towards commercial arrays of wave energy converters [4].

The waters of the Pentland Firth and Orkney are one of the key regions in the world suitable for exploitation of the marine renewable energy resource, where there are plans to develop 1.6 GW of wave and tidal energy capacity by 2020 [5], distributed among twelve leased sites (six wave and five tidal) [6] (Fig. 1), 550 MW of which are wave energy projects in Orkney waters (Table 1). Key to achieving this objective was the creation in 2004 of the European Marine Energy Centre (EMEC) [6] which, along with offering developers scaled sites for prototype testing, comprises a full-scale grid-connected inter-island channel tidal test site within the Orkney archipelago, and a full-scale grid-connected Atlantic-exposed wave test site to the west of Orkney (http://www.emec.org.uk). Although several accurate regional wave models exist of the Pentland Firth and Orkney waters [7–9], with one study considering time periods up to 20 years [10], these studies are either commercial, and so the results not publicly available, or have tended to focus on model validation, which includes significant calibration [10]. In particular, no study has yet attempted to quantify the wave resource of the region in relation to inter-annual, inter-seasonal, and spatial variability, and this has stimulated the present study. In addition to quantifying the wave power resource, such a study will also be useful to developers and researchers interested in tidal energy sites, since detailed knowledge of the wave climate is one of the variables affecting tidal stream site selection and operation [11].

Here, we use a high performance computing system to run high resolution wave model simulations, simulating the wave climate of the Pentland Firth and Orkney waters at high temporal resolution over a 10 year period, and so resolving inter-annual variability. The hydrography of the study region is introduced in Section 2, and the sources of data and wave modelling methodology, including validation, described in Section 3. The main results of the study are presented in Section 4, demonstrating the inter-annual and inter-seasonal variability of the wave power resource. In Section 5, the results are discussed in relation to variability of the NAO, and the theoretical *versus* practical resource assessed.

Table 1
Leased wave projects in Orkney waters. Data from The Crown Estate.

Site name	Capacity (MW)	Owner(s) of tenant
West Orkney South	50	E.ON Climate & Renewables UK Ltd
West Orkney Middle South	50	E.ON Climate & Renewables UK Ltd
Marwick Head	50	Scottish Power Renewables UK Ltd
Brough Head	200	Aquamarine Power Ltd & SSE Renewables Holdings (UK) Ltd
Costa Head	200	SSE Renewables Developments (UK) Ltd, Alstom UK Holdings Ltd
Billa Croo	n/a	European Marine Energy Centre (EMEC) Ltd

2. Hydrography of the study region

2.1. The North Atlantic

The UK climate is dominated by the polar front. The instability of this front causes depressions to form, which track across the North Atlantic and follow a preferred route between Iceland and Scotland [12]. Boreal winters in the northeast Atlantic are characterised by large long-period south-westerly to north-westerly waves, and summers are characterised by smaller shorter-period waves with a more northerly trend [13]. Considerable inter-annual variability in the synoptic-scale circulation over the North Atlantic is described by the North Atlantic Oscillation (NAO) index. The strong background flow results in high mean wave energy incident on the northwest European shelf seas, and the variability results in a wave climate with considerable extremes [14–16]. The NAO

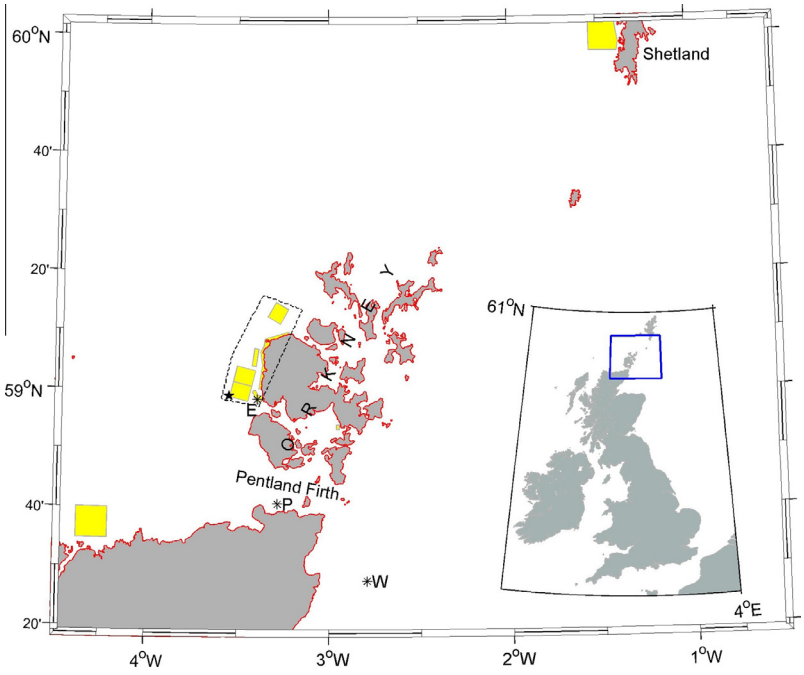

Fig. 1. Map of Pentland Firth and Orkney waters, showing UK Crown Estate leased wave sites (yellow shading) and (asterisks) the locations of the wave buoys used for model validation (E = EMEC, P = Pentland Firth, and W = Wick). The area enclosed by the dashed line to the west of Orkney is the 434km^2 (excluding land) region used for averaging. The black filled star shows the location of a theoretical Pelamis device, which forms the basis of the practical resource assessment in Section 5.2. Inset shows the location of Orkney in relation to the British Isles. (For interpretation of the references to colour in this figure legend, the reader is referred to the web version of this article.)

correlates well with the winter (December–January–February) wave power resource over the northwest European shelf seas [3]. Swell waves in the North Atlantic are mainly generated by intense extratropical cyclones which frequently originate in the western part of the North Atlantic east of Newfoundland, and move rapidly in a northeasterly direction [17].

2.2. Pentland Firth and Orkney

Orkney is an archipelago in the north of Scotland, separated from the Scottish mainland by the 12 km width of the Pentland Firth. Orkney is comprised of around 70 islands, separated by a series of bays and energetic tidal channels (Fig. 1). Orkney is mesotidal; however, tidal waves in the region, dominated by the principal semi-diurnal lunar (M_2) and solar (S_2) constituents, take around two and a half hours to propagate around Orkney from the western to the eastern approaches to the Pentland Firth, leading to a considerable phase lag across Orkney [18]. This phase lag results in a strong pressure gradient across Orkney, driving very strong tidal flows through the Pentland Firth and along the Firths of Orkney. The tidal currents flowing through the inter-island channels of Orkney exceed 3 m/s in many regions [19].

The deep water (water depth > 200 m) annual mean wave power resource to the west of Orkney is around 31 kW/m, reducing to 22 kW/m in the nearshore [20]. It has been demonstrated that the theoretical mean power output over an 8 year period at the EMEC wave test site for a 750 kW rated Pelamis device is 180 kW, with an uncertainty in measurements of order 10 kW [21]. A limited (34 day) summer wave model simulation of the Pentland Firth and Orkney waters demonstrates the distinct differences between the energetic Atlantic-dominated wave climate to the west of Orkney, in contrast to the relatively sheltered waters to the east [7]. Saruwatari et al. [7] also demonstrate that the peak tidal currents in the Pentland Firth (of order 3 m/s) can impact the summer wave resource by up to 60% due to wave–current interaction. However, it should be noted that such impacts are considerably greater for shorter period waves experienced during summer months, than would be the case for longer period winter waves [22], and hence wave–current interaction is likely to have a relatively modest contribution to the wave power resource when extended to annual timescales, which are dominated by the more energetic autumn/winter months.

3. Wave modelling

Here, the spectral wave model SWAN is used to simulate the Orkney wave power resource over a ten year period. Neglecting tidal effects, the SWAN wave model requires wind and bathymetry inputs, described in the following two subsections, followed by a description of the wave model, model implementation, and validation.

3.1. Wind data

The source of synoptic surface wind fields used to force the wave model was the ECMWF-ERA-Interim reanalysis [23], available at a (global) grid resolution of $0.75^\circ \times 0.75^\circ$, 3-hourly from 1979 to 2013. The ERA-Interim analysis differs from previous reanalysis products (i.e. ERA-15 and ERA-40) in that it includes 4D-Var (or data assimilation in time as well as all three spatial dimensions), and has improved horizontal resolution (T255 $\sim$ 80 km in contrast to T159 $\sim$ 125 km for ERA-40). In addition to the data being available to the user at a higher resolution than previous ERA-40 and ERA-15 datasets, the original analysis is also at a better resolution, hence the standard gridpoint data should improve the representation of the observed atmosphere. The ERA-Interim wind fields have been successfully applied to a range of marine renewable energy studies, including simulations of the wave climate in the Black Sea [24], and the Canary Islands [25].

3.2. Bathymetry data

Bathymetry data for both scales of model simulation (the outer North Atlantic model and the inner nested regional Pentland Firth and Orkney waters model) were bi-linearly interpolated from the GEBCO (General Bathymetric Chart of the Oceans) $1/120^\circ \times 1/120^\circ$ gridded bathymetry dataset, distributed by BODC (the British Oceanographic Data Centre). The GEBCO data was generated by combining quality-controlled ship depth soundings with interpolation between sounding points guided by satellite-derived gravity data. However, in regions where there was an improvement on the existing grid, data sets generated by other methods were also included.

3.3. SWAN wave model

The third-generation spectral wave model SWAN (Simulating Waves Nearshore) was used to simulate wave climates over the North Atlantic, and the waters of the Pentland Firth and Orkney. SWAN has been used successfully in many wave power resource studies spanning a range of scales, such as the northwest European shelf seas [3], the Oregon coast [26], and the Death Coast of Spain [27]. SWAN is an Eulerian formulation of the discrete wave action balance equation [28]. The model is spectrally discrete in frequencies and directions, and the kinematic behaviour of the waves is described by the linear theory of gravity waves. SWAN accounts for wave generation by wind, non-linear wave-wave interactions, white-capping, and the shallow water effects of bottom friction, refraction, shoaling, and depth-induced wave breaking.

The evolution of the action density ($N = E/\sigma$) is governed by the wave action balance equation which, in spherical coordinates, is [28]

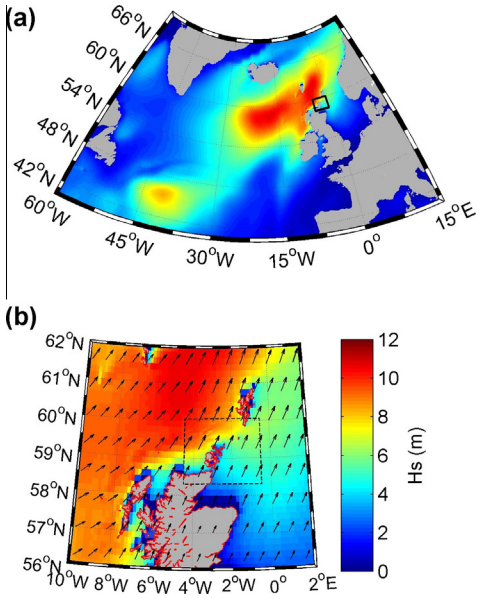

Fig. 2. Scales of nesting for the SWAN model simulations. (a) Outer North Atlantic model and (b) interface between coarser North Atlantic model and (boxed) inner nested higher resolution Pentland Firth and Orkney waters model. The vectors in (b) show the spatial resolution of the corresponding ERA-Interim wind field, and the colour scale is a typical snapshot of significant wave height (10 January 2009, 12:00), with the colour bar shown in (b) common to both sub-figures. (For interpretation of the references to colour in this figure legend, the reader is referred to the web version of this article.)

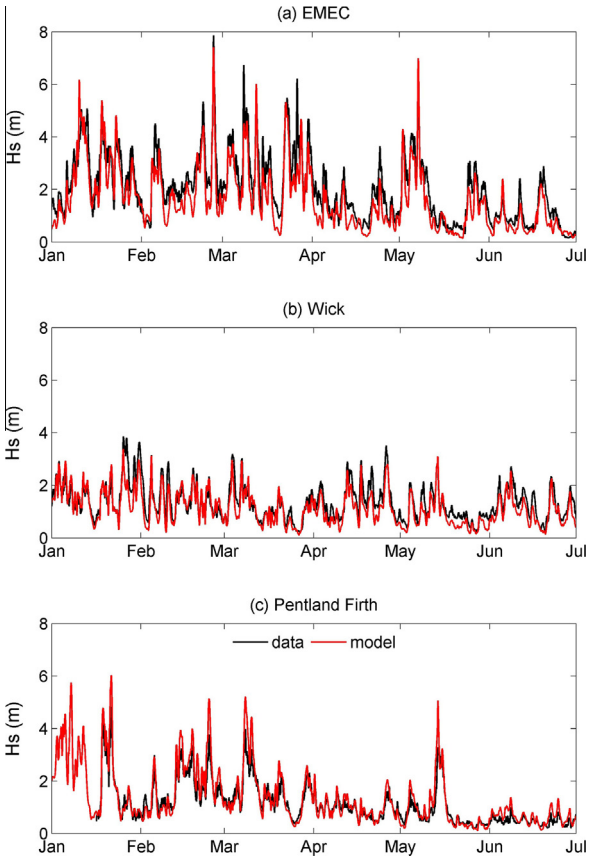

Fig. 3. Six month time series of observed and simulated significant wave height (Hs) at the 3 validation stations. In (a), the time period is January–June 2009, and in (b) and (c), the time period is January–June 2012.

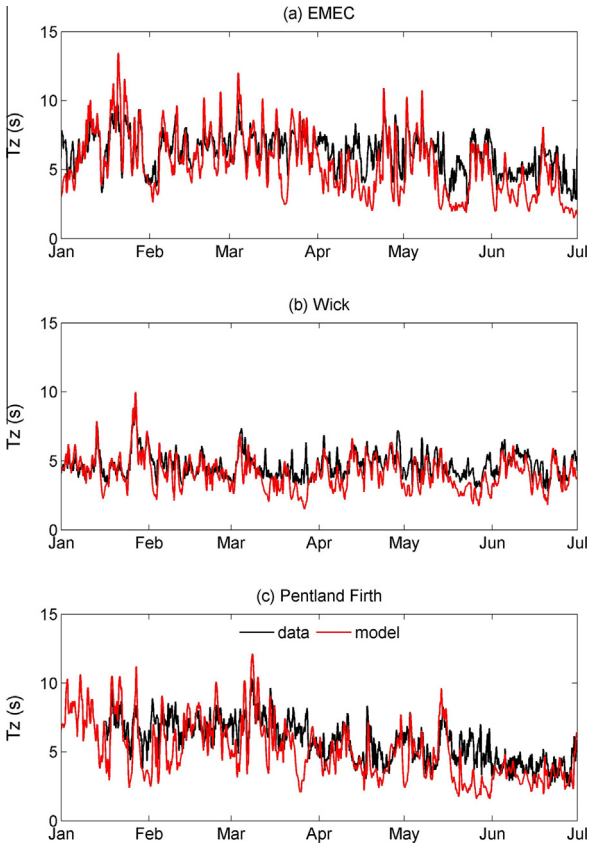

Fig. 4. Six month time series of observed and simulated zero upcrossing wave period (Tz) at the 3 validation stations. In (a), the time period is January–June 2009, and in (b) and (c), the time period is January–June 2012.

$$\frac{\partial N}{\partial t}+\frac{\partial c_\lambda N}{\partial \lambda}+\frac{\partial c_\phi N}{\partial \phi}+\frac{\partial c_\sigma N}{\partial \sigma}+\frac{\partial c_\theta N}{\partial \theta}=\frac{S_{tot}}{\sigma} \quad (1)$$

where E is spectral energy density, σ is angular frequency, θ is wave direction, c_λ and c_ϕ are the propagation velocities in the zonal (λ) and meridional (ϕ) directions, c_σ and c_θ are the propagation velocities in spectral space, and S_{tot} represents the source terms, i.e. generation, dissipation, and non-linear wave-wave interactions. In application to the North Atlantic, the wave energy spectrum at each grid point was divided into 40 discrete frequency bins and 45 discrete direction bins. For the Pentland Firth and Orkney regional model, the number of discrete direction bins was increased to 90 to minimise the so called garden sprinkler effect [29], which was particularly apparent in the relatively low energy region to the east of the Pentland Firth. The lowest modelled frequency was 0.04 s^{-1} (period $T = 25$ s), and the highest frequency resolved by the model was 2 s^{-1} ($T = 0.5$ s). Outside of this range, the wave spectrum was imposed, hence the effects of lower and higher frequencies are also included in the simulations [30].

Version 40.85 of SWAN was run in third-generation mode, with Komen linear wave growth and whitecapping, and quadruplet wave-wave interactions. SWAN default formulations and coefficients were used for all of the physical processes.

3.4. Model implementation

The wave model was applied initially to a region which covered the entire North Atlantic at a grid resolution of $1/6^\circ \times 1/6^\circ$, extending from 60°W to 15°E, and from 40°N to 70°N (Fig. 2a). Since the limits of this outer nest were sufficiently distant from the region of interest (the north of Scotland), the incoming wave components at this outer boundary were set to zero when waves propagated from the boundary towards the interior, or with the computed outgoing wave components when waves propagated from the interior towards the boundary. Two-dimensional (2D)

Table 2
Model validation statistics at the three wave buoys.

Location	Time period	*Hs*			*Tz*		
		RMSE[1] (m)	SI[2]	ρ[3]	RMSE[1] (s)	SI[2]	ρ[3]
EMEC	1/1/2009–30/6/2009	0.61	0.30	0.93	1.65	0.27	0.77
Wick	1/1/2012–30/6/2012	0.38	0.28	0.89	0.99	0.21	0.72
Pentland Firth	17/1/2012–30/6/2012	0.38	0.34	0.95	1.73	0.30	0.69

[1] Root-mean-squared-error.
[2] Scatter index (RMSE normalised by the mean of the observations).
[3] Pearson's linear correlation coefficient at 95% confidence level.

wave spectra were output hourly from this coarse outer grid simulation and interpolated to the boundary of an inner nested high resolution model of the Pentland Firth and Orkney waters (Fig. 2b). This inner nested region had a grid resolution of $1/120^\circ \times 1/234^\circ$ (approximately 434 m), extending from 4°30′W to 0°30′W, and from 58°18′N to 60°03′N (the region shown in Fig. 1). After running the coarser outer model of the North Atlantic, this inner nested simulation was run without feedback to the outer nest, i.e. the nesting process was one-way. It should be noted that many wave modelling studies [e.g. 31] use many levels of nesting to transfer wave properties from ocean basin to shelf scale. Although there are no specific guidelines on levels of nesting in SWAN, the nesting process should be capable of capturing spatial variations along the boundary, and to adequately resolve the coastline. Examining Fig. 2b by way of example, the nesting process has adequately captured such processes for this extreme event, but one should perhaps be cautious when interpreting model outputs in the southwest of the inner nested region, since wave refraction will not be fully resolved at the boundary by the outer nested model. Wave power **P** (the flux of wave energy), is a vector quantity, and was calculated from the full wave spectrum using,

$$\mathbf{P} = \iint \mathbf{c_g}(\sigma, d) E(\sigma, \theta) \mathrm{d}\sigma \, \mathrm{d}\theta \tag{2}$$

output every 3 h from the inner nested simulation at every grid point, where $\mathbf{c_g}(\sigma, d)$ is the wave group celerity vector, and d is water depth. In addition, hourly values of significant wave height (Hs) and zero upcrossing wave period (Tz) were output at selected stations for model validation (Section 3.5). The models were run for a 10 year period (2003–2012), a decade which witnessed considerable variability in the NAO, and hence contained considerable inter-annual variability with which to examine extremes in the wave climate.

The coarser North Atlantic wave model took around 700 CPU hours for each year of simulation, using 96 × 2.9 GHz Intel Xeon Sandy Bridge cores. The higher resolution inner-nested regional Pentland Firth and Orkney model (which had double the directional discretisation as the outer model) took around 23,160 CPU hours per year of simulation using the same high performance computing system. The scale of the technical and computational challenges of running a wave model at the scale of this study for a decade of high spatial, temporal and spectral resolution should therefore not be underestimated.

3.5. Model validation

The model was validated over a six month period against half-hourly wave data obtained from three wave buoys (Fig. 1) – one to the west of Orkney (EMEC), one in the Pentland Firth, and one to the southeast of the Pentland Firth (Wick). Time series of significant wave height Hs at the 3 validation locations are given in Fig. 3, and the corresponding validation statistics provided in Table 2. Time series of zero upcrossing wave period Tz at the 3 validation locations are given in Fig. 4, with the corresponding validation statistics also provided in Table 2. There is evidence of strong wave–current interaction in most of the variables in the wave buoy data, particularly in the Pentland Firth, where our FFT analysis (not shown) revealed peaks in the power spectrum at semi- and quarter-diurnal frequencies (i.e. the frequencies related to the vertical and horizontal tides, respectively). To examine the wave resource of the Pentland Firth in more detail would require a coupled wave-tide model. However, the time series and statistics from our model validation (e.g. RMSE ~ 0.5 m for Hs, and ~1.5 s for Tz, Table 2) indicate that a wave-only model is an appropriate tool to examine the regional wave resource at the spatial and temporal scales of our study, particularly considering the computational expense of running a fully coupled model for a decade of simulation.

4. Results

The annual cycle of monthly mean wave power resource averaged over all 10 years of model simulations demonstrates clearly the seasonal variability of the resource (Fig. 5), with a stronger (~30–50 kW/m) resource to the north and west of Orkney during

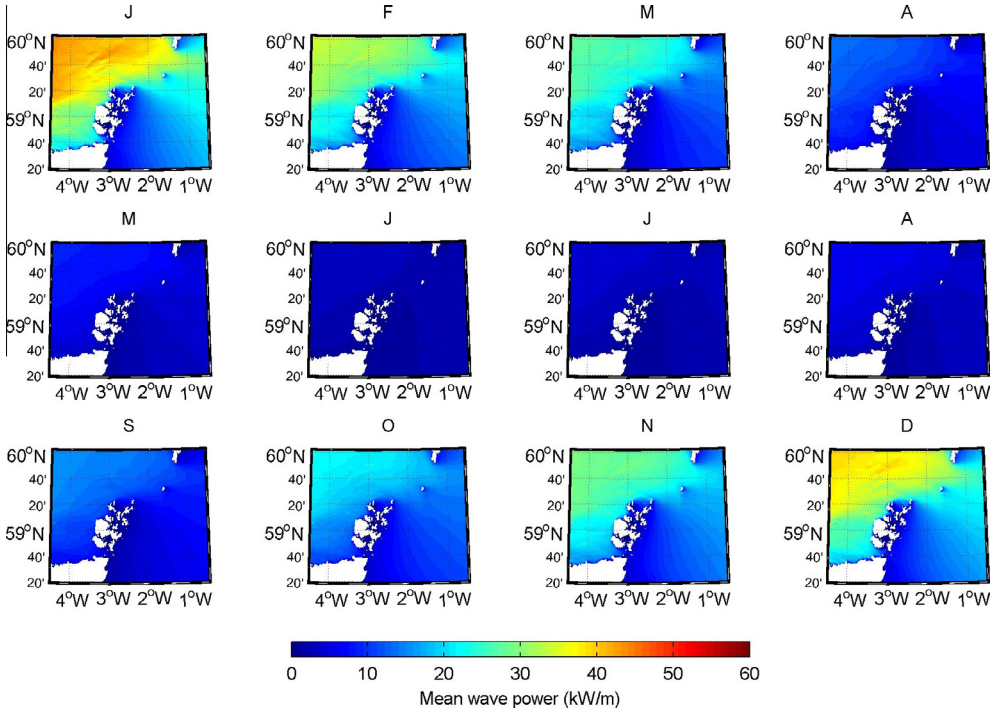

Fig. 5. Annual cycle of monthly mean wave power averaged over all 10 simulated years.

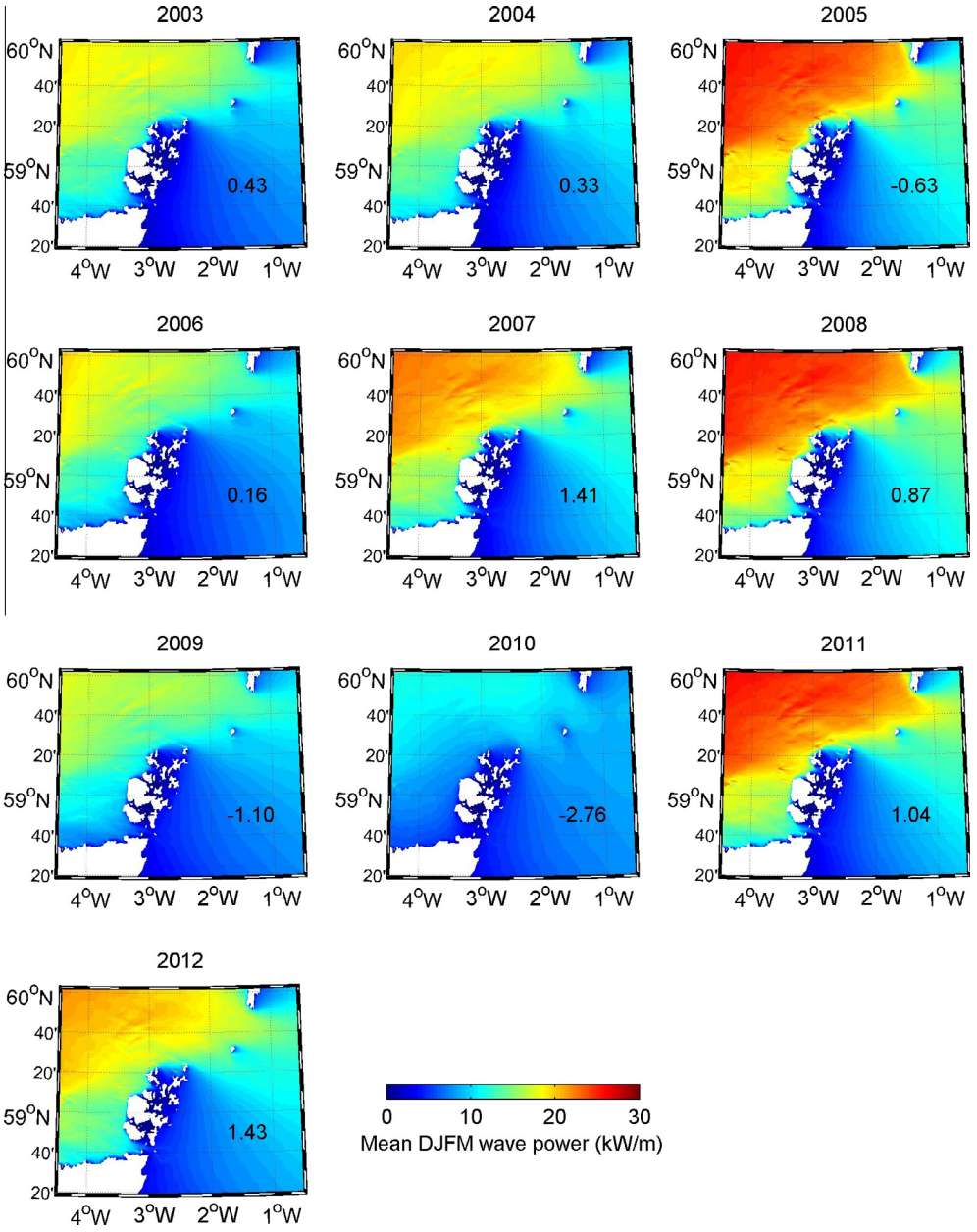

Fig. 6. Inter-annual variability of the DJFM wave power resource. Values on the plots are DJFM NAO for each year.

winter months, reducing to <10 kW/m during summer months. The largest resource was generally located to the north of Orkney, with a significant resource to the west, and minimal resource (<15 kW/m throughout the year) to the east of Orkney. Examining the variability of the extended winter (DJFM) resource in more detail (Fig. 6), there is strong inter-annual variability, with the winter month resource to the north and west of Orkney ranging from around 10 kW/m in 2010 to around 20–25 kW/m in 2005, 2008 and 2011. Although discussed in more detail in Section 5.1, this inter-annual variability can be linked to the DJFM NAO, which was strongly negative (−2.76) in 2010, and generally strongly positive during more energetic winters. If the mean wave power resource is examined in more detail within the averaging region to the west of Orkney (shown in Fig. 1 as the region bounded by a dashed line which encompasses all of the Orkney Crown Estate leased wave sites), the seasonal variability in the mean wave resource is associated with a seasonal variability in the uncertainty, shown here as the 90% confidence intervals and the range (Fig. 7). In the most energetic and variable month, January, mean wave power was 30.5 ± 10.4 kW/m. In contrast, the least energetic month, July, is characterised by a mean wave power resource of 3.7 ± 0.6 kW/m. Dividing the model results into seasons, the spatial distribution of seasonal and annual mean wave power resource, and uncertainty in the resource can be calculated (Fig. 8). When expressed as a percentage, there is relatively low ($\sim 30\%$) uncertainty to the west of Orkney during winter months, increasing to $\sim 40\%$ during autumn months. In contrast, there is high uncertainty ($\sim 60\%$) in the modest resource to the east of Orkney during winter months, which reduces to $\sim 35\%$ in the autumn.

Detailed contour plots of the monthly mean wave power resource for each year of the simulated decade are presented in the Supplementary material.

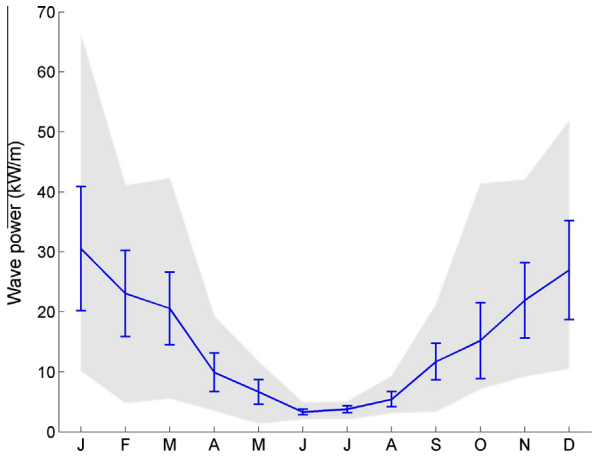

Fig. 7. Annual cycle of monthly mean wave power for a 434 km^2 region to the west of Orkney. Error bars show 90% confidence intervals, and grey shading indicates range.

5. Discussion

A high resolution decade of wave model simulations demonstrates the large variability of the wave power resource around Orkney, with a winter variability of around 30% to the west of Orkney. The results highlight the marked differences between the wave resource to the west and east of Orkney, with the latter exhibiting considerably more winter variability (60%), in relation to a relatively low winter mean wave resource (10 kW/m).

5.1. North Atlantic Oscillation

The North Atlantic Oscillation (NAO) is a major source of inter-annual variability in the atmospheric circulation, associated with changes in the surface westerlies across the North Atlantic [32]. Wave power in the study region has previously been linked to the NAO [3,33,34], particularly over winter months. In order to determine the time period during which such a correlation is strongest for the study region, the Pearson linear correlation coefficient (ρ) between monthly wave power to the west of Orkney, and monthly NAO was calculated (Fig. 9). The time period of consecutive months with a significance level of greater than 90% was DJFM, and hence this extended winter period was used for more detailed analysis.

DJFM wave power to the west of Orkney correlates well with the DJFM NAO, with a significant linear coefficient of determination $r^2 = 0.57$ (at the 95% confidence level), for $n = 9$ (Fig. 10). The relationship is positive; hence an extended winter period with a strongly positive NAO (i.e. a winter that is characterised by stronger westerlies [32]) corresponds to a high (>35 kW/m) wave resource to the west of Orkney. In contrast, a strongly negative NAO winter (i.e. a winter that is characterised by weaker winds) corresponds to a relatively low (<15 kW/m) wave resource.

There were several extreme values of the DJFM NAO encountered during the selected decade of simulation, e.g. the strongly negative DJFM NAO of 2009/2010, and the strongly positive years 2006/2007 and 2011/2012 (Fig. 10). To determine whether such extremes are typical within decadal timescales, longer term trend analysis of the DJFM NAO over the period 1825–2012 was performed (Fig. 11a). Qualitatively, it does appear that strongly negative NAO winters have become more frequent over time (e.g.

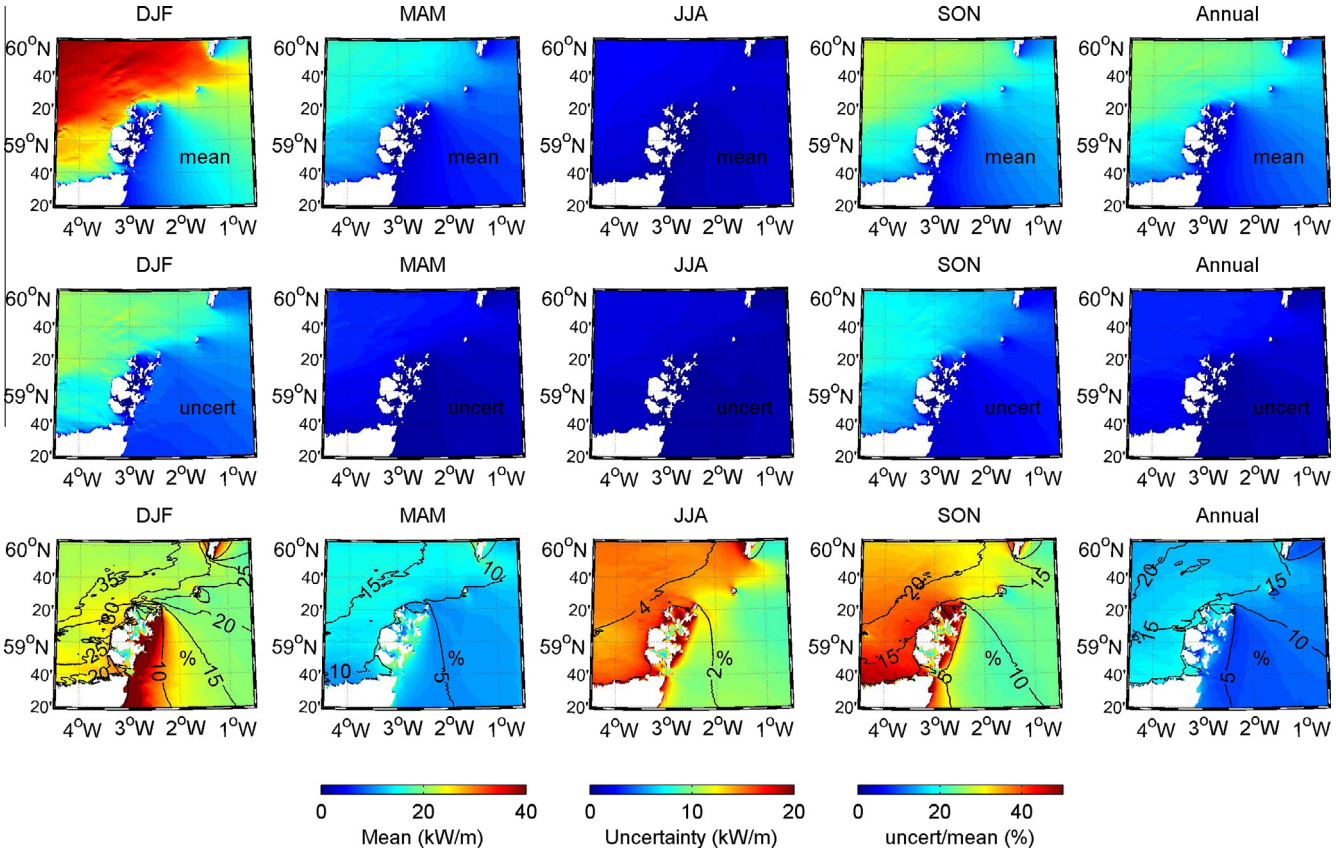

Fig. 8. Annual and seasonal distribution of mean wave power, wave power uncertainty (90% confidence), and uncertainty expressed as a percentage of mean wave power. Contour values on the bottom panels show mean wave power.

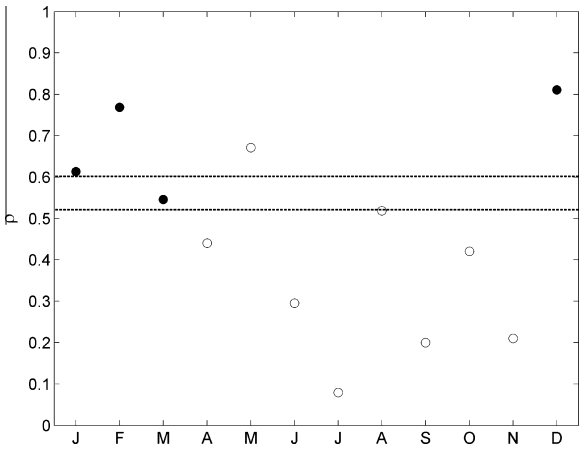

Fig. 9. Pearson's linear correlation coefficient (ρ) between monthly wave power to the west of Orkney, and monthly NAO. Lower dashed line represents the 90% significance level, and the upper dashed line indicates 95% significance. Filled circles are months selected for more detailed NAO analysis.

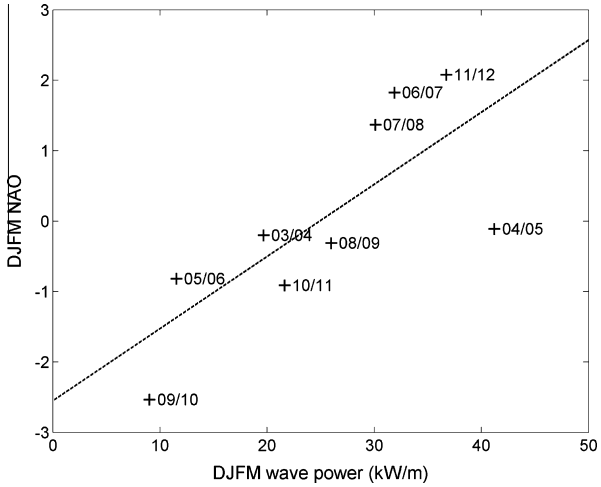

Fig. 10. Mean winter (December–January–February–March) wave power to the west of Orkney plotted against the DJFM NAO. Labels yy/yy associated with each point on the graph indicates the two years spanned by each DJFM period. The dashed line is the least squares line of best fit ($r^2 = 0.57$).

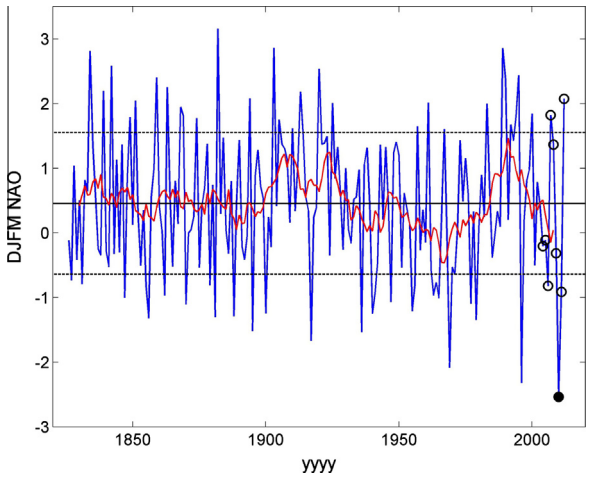

Fig. 11. Trend in DJFM NAO from 1825 to 2012. The red line shows the ten year rolling average. Circles indicate the decade used in this study (2003–2012), and the filled circle is the 2009/2010 anomaly (strongly negative NAO). The solid horizontal line is the mean, and dashed lines indicate one standard deviation from the mean. (For interpretation of the references to colour in this figure legend, the reader is referred to the web version of this article.)

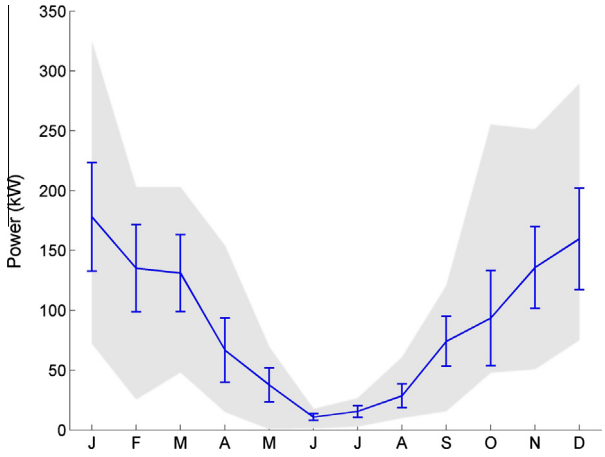

Fig. 12. Annual cycle of monthly mean power output for a 750 kW Pelamis device located to the west of Orkney (location is shown in Fig. 1). Error bars show 90% confidence intervals, and grey shading indicates range.

1968/1969, 1995/1996 and 2009/2010), and therefore any recent 10 year hindcast is likely to include one of these events. Further, it appears that the decade of simulation selected for this study (2003–2012) was relatively typical of any recent decade hindcast in terms of the DJFM NAO, as can be seen from the 10 year rolling average of the DJFM NAO (red line in Fig. 11), which falls well within one standard deviation of the mean. However, to provide a more robust relationship between wave power and NAO would require a longer simulation period to fully resolve the inter-decadal variability within the NAO.

There is some debate in the scientific community about how the NAO will change in the future, as a consequence of climate change [35]. Such debates are relevant to the European wave energy research community, since the sign and magnitude of the NAO correlates well with the wave energy resource (Fig. 10). The WASA Group [36] found no significant future changes in storm activity and wave height in the northeast Atlantic, whereas Debernard and Røed [37] found a future decrease in wave height. However, there is much uncertainty in future patterns of storminess estimated by climate models due to parameterization of sub-grid scale processes and the time-slice approach used for such studies [38]. In addition, Allan et al. [39] found that inter-annual variability has become a prominent feature over the British Isles during the latter half of the twentieth century. Therefore, before we can meaningfully estimate how the wave power resource will vary in the future, for example through extending the model simulations presented here to provide a more robust relationship between wave power and the NAO, there first needs to be consensus from the climate change research community.

5.2. Practical wave resource

So far, the analysis and discussion of variability has focussed on the theoretical resource. In order to estimate variability of the practical wave resource, the ten year modelled time series of *Hs* and energy wave period *Te* was applied to the published power matrix of a single 750 kW Pelamis device [21], for a site to the west of Orkney located at the Atlantic limit of the 50 MW E.ON leased wave site (Fig. 1). Wave direction was neglected in the calculation, since the Pelamis device is designed to align itself with the direction of highest wave power [1]. The resulting annual cycle of monthly mean power output is shown in Fig. 12 (which can be contrasted to the annual cycle in the theoretical resource, Fig. 7).

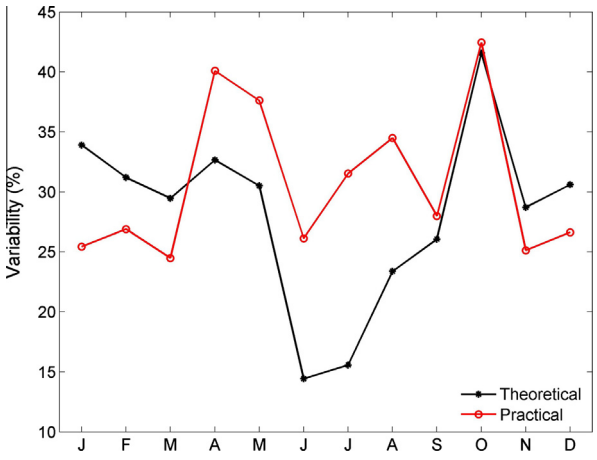

Fig. 13. Percentage variability of the theoretical and practical wave resource to the west of Orkney for all ten years of simulation.

Examining the month during which the wave power was highest (January), mean power extracted by a Pelamis device was 178.1 ± 45.3 kW/m, with the variability (at a 90% confidence level) representing around 25% of the mean. In contrast, the theoretical January resource was 30.5 ± 10.4 kW/m (Fig. 10), with the variability representing around 34% of the mean. Extending this analysis to all months (Fig. 13), a trend develops in which the percentage variability in the November–March practical resource is less than the variability in the theoretical resource. In contrast, variability in the April–October practical resource is greater than the variability of the theoretical resource. Winter variability in the practical resource is moderated by the Pelamis power matrix. In particular, the Pelamis device enters survival mode when $Hs > 8$ m, which occurred for around 100 h to the west of Orkney during the simulated decade. Since a large amount of wave energy is contained within these wave heights, and the wave power of such large waves are not exploited by the majority of wave devices, this leads to a considerable over-estimate of the theoretical resource of a region, and the associated variability, in contrast to the practical resource. Developers of future generations of wave devices (or arrays of devices) might therefore wish to exploit both mean and extreme waves to maximise electricity generation. This could be achieved, for example, by developing devices that can operate during storm events, possibly working in concert within an array of devices which are tuned to exploit the less energetic, but more frequent, mean waves.

6. Conclusions

High resolution wave model simulations were generated to investigate the temporal variability of the wave resource around Orkney, demonstrating that there was around 30% winter variability of the resource to the west of Orkney over the decade of simulations (2003–2012) – a decade that was representative of longer timescale inter-annual variability of the resource. Analysis of the model outputs demonstrated that the winter wave power resource over this decade correlates well with the North Atlantic Oscillation; however, a longer time period of simulations would be required to fully resolve inter-decadal variability. The power matrix for a 750 kW Pelamis device was applied to the model outputs to estimate variability of the practical wave resource over the simulated decade, demonstrating that during winter months, there was less variability in the practical resource in comparison to variability of the theoretical resource. This is because a large contribution to wave variability is contained within relatively few large winter events, yet the Pelamis device enters survival mode during such events, hence the variability of these events is not reflected in the Pelamis power output. In the Supplementary material, detailed month-by-month wave power resource maps are provided of the simulated decade to assist developers and other researchers in estimating spatial and temporal variability of the Orkney wave resource.

This study made use of 3-hourly wind forcing from the ERA-Interim dataset at $0.75^\circ \times 0.75^\circ$ spatial resolution to force a wave model. Although this is adequate for this study (examining variability over a decade), and is a widely used and much respected dataset, for individual events or for higher resolution coastal models, it would be useful to consider high frequency temporal variability [40], and to consider spatial resolution of wind forcing which accounts for topographic effects. In relation to spatial resolution – although the model resolution used was state-of-the-art (around 434 m) considering the extent of the study region, if wave-tide interactions and nearshore processes were to be included, increased spatial resolution would be important, particularly in regions which experience rapid changes in bathymetry or high tidal flows. Developers interested in, for example, the wave climate of northwest mainland Scotland may require an intermediate nesting stage, to better resolve waves generated in the North Atlantic and their evolution into this shallow region. However, it is important to match any increased model resolution to the availability of high resolution bathymetry data. An examination of how variability affects different wave frequencies would be complementary to this study, since this would allow device/site developers to either tune or select their technology to capitalise on the regions of the wave spectrum which experience the lowest inter-annual and inter-seasonal variability. Finally, although a decade of simulations at high resolution was already a demanding computational task, it would be interesting to extend such a study to longer time periods, particularly to examine inter-decadal trends in the wave climate through climatic indices such as the NAO.

Acknowledgements

Thanks to Philippe Gleizon (University of the Highlands and Islands, Thurso) for providing wave buoy data, Tim Osborn (University of East Anglia) for providing monthly NAO data, and the ECMWF for providing synoptic wind fields from the ERA-Interim dataset. We acknowledge the support of High Performance Computing Wales (HPCW), a collaboration between all the universities in Wales, the European Regional Development Fund (ERDF), the European Social Fund (ESF), and Fujitsu, for access to supercomputing facilities, and we particularly wish to thank Ade Fewings of HPCW for his support in setting up and optimising the wave model. We also thank two anonymous reviewers whose constructive feedback on an earlier version of the manuscript helped improve the final accepted version of the paper. SPN and MJL acknowledge the support of the UK Engineering and Physical Sciences Research Council (EPSRC) through SuperGen project EP/J010200/1, and MRH acknowledges the support of the SEACAMS project, funded by ERDF and ESF.

Appendix A. Supplementary material

Supplementary data associated with this article can be found, in the online version, at http://dx.doi.org/10.1016/j.apenergy.2014.07.023.

References

[1] Gunn K, Stock-Williams C. Quantifying the global wave power resource. Renew Energy 2012;44:296–304.
[2] Arinaga RA, Cheung KF. Atlas of global wave energy from 10 years of reanalysis and hindcast data. Renew Energy 2012;39:49–64.

[3] Neill SP, Hashemi MR. Wave power variability over the northwest European shelf seas. Appl Energy 2013;106:31–46.
[4] Clement A, McCullen P, Falcao A, Fiorentino A, Gardner F, Hammarlund K, et al. Wave energy in Europe: current status and perspectives. Renew Sustain Energy Rev 2002;6:405–31.
[5] Allan G, Lecca P, McGregor P, Swales J. The economic impacts of marine energy developments: a case study from Scotland. Mar Policy 2014;43:122–31.
[6] Johnson K, Kerr S, Side J. Accommodating wave and tidal energy – control and decision in Scotland. Ocean Coast Manage 2012;65:26–33.
[7] Saruwatari A, Ingram DM, Cradden L. Wave–current interaction effects on marine energy converters. Ocean Eng 2013;73:106–18.
[8] Bertotti L, Cavaleri L. Modelling waves at Orkney coastal locations. J Mar Syst 2012;96–97:116–21.
[9] Venugopal V, Smith GH. Wave climate investigation for an array of wave power devices. In: Proceedings of the 7th European wave and tidal energy conference, Porto, Portugal; 2007. p. 1–10.
[10] Lawrence J, Chevalier C. High-resolution metocean modelling at EMEC's (UK) marine energy test sites. In: Proceedings of the 8th European wave and tidal energy conference, Uppsala, Sweden; 2009. p. 1–13.
[11] Lust EE, Luznik L, Flack KA, Walker JM, Van Benthem MC. The influence of surface gravity waves on marine current turbine performance. Int J Mar Energy 2013;3-4:27–40.
[12] Palutikof J, Holt T, Skellern A. Wind: resource and hazard. In: Hulme M, Barrow E, editors. Climates of the British Isles: past present and future. Routledge; 1997. p. 220–42.
[13] Dodet G, Bertin X, Taborda R. Wave climate variability in the North-East Atlantic Ocean over the last six decades. Ocean Model 2010;31:120–31.
[14] Draper L. Wave climatology of the U.K. continental shelf. In: Banner F, Collins M, Massie K, editors. The north-west European shelf seas: the sea bed and the sea in motion. Physical and chemical oceanography and physical resources, vol. II. Elsevier; 1980. p. 353–68.
[15] Neill SP, Scourse JD, Bigg GR, Uehara K. Changes in wave climate over the northwest European shelf seas during the last 12,000 years. J Geophys Res 2009;114:C06015.
[16] Neill SP, Scourse JD, Uehara K. Evolution of bed shear stress distribution over the northwest European shelf seas during the last 12,000 years. Ocean Dyn 2010;60:1139–56.
[17] Gjevik B, Krogstad HE, Lygre A, Rygg O. Long period swell wave events on the Norwegian shelf. J Phys Oceanogr 1988;18:724–37.
[18] Neill SP, Hashemi MR, Lewis MJ. The role of tidal asymmetry in characterizing the tidal energy resource of Orkney. Renew Energy 2014;68:337–50.
[19] Bryden IG, Couch SJ. ME1 marine energy extraction: tidal resource analysis. Renew Energy 2006;31:133–9.
[20] Folley M, Whittaker T. Analysis of the nearshore wave energy resource. Renew Energy 2009;34:1709–15.
[21] Mackay EB, Bahaj AS, Challenor PG. Uncertainty in wave energy resource assessment. Part 1: Historic data. Renew Energy 2010;35:1792–808.
[22] Hashemi MR, Neill SP. The role of tides in shelf-scale simulations of the wave energy resource. Renew Energy 2014;69:300–10.
[23] Dee DP, Uppala SM, Simmons AJ, Berrisford P, Poli P, Kobayashi S, et al. The ERA-Interim reanalysis: configuration and performance of the data assimilation system. Quart J Roy Meteorol Soc 2011;137:553–97.
[24] Akpnar A, Kömürcü Mh. Assessment of wave energy resource of the Black Sea based on 15-year numerical hindcast data. Appl Energy 2013;101:502–12.
[25] Gonçalves M, Martinho P, Guedes Soares C. Assessment of wave energy in the Canary Islands. Renew Energy 2014;68:774–84.
[26] García-Medina G, Özkan Haller HT, Ruggiero P. Wave resource assessment in Oregon and southwest Washington USA. Renew Energy 2014;64:203–14.
[27] Iglesias G, Carballo R. Wave energy potential along the Death Coast (Spain). Energy 2009;34:1963–75.
[28] Booij N, Ris RC, Holthuijsen LH. A third-generation wave model for coastal regions – 1. Model description and validation. J Geophys Res 1999;104:7649–66.
[29] Tolman HL. Alleviating the garden sprinkler effect in wind wave models. Ocean Model 2002;4:269–89.
[30] Holthuijsen LH. Waves in oceanic and coastal waters. Cambridge University Press; 2009.
[31] Zacharioudaki A, Pan S, Simmonds D, Magar V, Reeve DE. Future wave climate over the west-European shelf seas. Ocean Dyn 2011;61:807–27.
[32] Hurrell JW. Decadal trends in the North Atlantic Oscillation: regional temperatures and precipitation. Science 1995;269:676–9.
[33] Mackay EB, Bahaj AS, Challenor PG. Uncertainty in wave energy resource assessment. Part 2: Variability and predictability. Renew Energy 2010;35:1809–19.
[34] Tsimplis MN, Woolf DK, Osborn TJ, Wakelin S, Wolf J, Flather R, et al. Towards a vulnerability assessment of the UK and northern European coasts: the role of regional climate variability. Philos Trans Ser A, Math Phys Eng Sci 2005;363:1329–58.
[35] Wang XL, Zwiers FW, Swail VR. North Atlantic Ocean wave climate change scenarios for the twenty-first century. J Clim 2004;17:2368–83.
[36] WASA. Changing waves and storms in the northeast Atlantic? Bull Am Meteorol Soc 1998;79:741–60.
[37] Debernard JB, Røed LP. Future wind, wave and storm surge climate in the Northern Seas: a revisit. Tellus 2008;60A:427–38.
[38] Lewis M, Horsburgh K, Bates P, Smith R. Quantifying the uncertainty in future coastal flood risk estimates for the U.K.. J Coast Res 2011;27:870–81.
[39] Allan R, Tett S, Alexander L. Fluctuations in autumn – winter severe storms over the British Isles: 1920 to present. Int J Climatol 2009;371:357–71.
[40] Goward Brown AJ, Neill SP, Lewis MJ. The influence of wind gustiness on estimating the wave power resource. Int J Mar Energy 2013;3–4:e1–10.